LO-phonon-enhanced microcavity polariton emission

S. Pau, G. Björk, H. Cao, F. Tassone, R. Huang, and Y. Yamamoto
Edward L. Ginzton Laboratory, Stanford University, Stanford, California 94305

R. P. Stanley
IMO-DP, Ecole Polytechnique Fédérale de Lausanne (EPFL), Lausanne CH1015, Switzerland
(Received 11 November 1996)

We observe resonant enhancement of the microcavity exciton-polariton emission by more than three orders of magnitude when the excitation laser is tuned to a single longitudinal-optical-phonon energy above the polariton energies. Our finding provides a scheme to efficiently populate $k_{\|}=0$ polaritons which bypasses the slow-acoustic-phonon thermalization process.
[S0163-1829(97)51104-0]

Microcavity light emitting devices based on quantum well excitons as a gain medium have the potential of being very fast because of the fast ($\sim$10 ps) exciton radiative lifetime[1] and of having high quantum efficiency because of microcavity confinement.[2] Nevertheless, in practice the speed of such devices is slow because of slow carrier thermalization time of the order of 200 to 500 ps. Since only the $k_{\|}\simeq 0$ (in plane k vector) exciton is optically active, hot excitons with large $k_{\|}$ must first thermalize before emission of radiation. For any current injection device which initially creates hot excitons, the slow thermalization time severely limits the performance of the device. The problem is how to efficiently and rapidly populate $k_{\|}\simeq 0$ optically active excitons. One possible solution is to inject carriers at one longitudinal-optical (LO)-phonon energy above the exciton resonance since the electron-LO phonon scattering time is subpicosecond.[3]

Recently enhanced Raman scattering in a planar semiconductor microcavity has been observed where the excitation laser is tuned below the lowest-order heavy-hole exciton transition (virtual excitation Raman scattering).[4] The enhancement of the light-matter interaction by the presence of the microcavity should lead not only to an enhanced Raman cross section for the virtual excitation but also should lead to enhanced Raman transition for real excitation at above the resonance. The real excitation with LO-phonon emission is particularly interesting for the applications to enhanced spontaneous emission coupling efficiency[2] β and exciton-polariton boser[5] because of its high-energy selectivity and large cross section. The normal modes of the microcavity system in a strong coupling regime are the microcavity exciton polaritons.[6,7] In this paper we report the first experimental result showing enhanced polariton emission where the excitation laser is tuned one LO-phonon energy above the $k_{\|}=0$ microcavity polariton energy. Aside from the increase in emission intensity caused by the LO-phonon resonance condition of the microcavity, we find that (i) selective excitation of upper- and lower-energy polariton branches can be achieved by tuning the laser wavelength, (ii) unlike the bulk, the LO-phonon line is strongly angular dependent due to the microcavity polariton dispersion effect, and (iii) the competition of acoustic and LO-phonon relaxation processes is evident in the polariton PL spectra at low temperature.

The microcavity sample is grown by molecular-beam epitaxy and has 19 (30) pairs of Bragg reflectors made of $Al_{0.15}Ga_{0.85}As$ and AlAs on top (bottom) and a single 20 nm GaAs quantum well (QW) at the center of the λ cavity. The $Al_{0.3}Ga_{0.7}As$ cavity buffer layer is tapered in one direction so that the cavity resonance energy varies with sample position, while the QW exciton energy is constant. Reflectivity and photoluminescence (PL) measurements are made at 4.5 K with a tungsten lamp and a CW tunable single mode Ti:sapphire ring laser, respectively. Both the laser and the white light passed through a 10 μm diameter pinhole that is imaged (1:2) onto the sample at an angle θ from the normal direction. Reflectivity is measured at normal incidence ($\theta=0$). Emission is collected at an angle α from the cavity normal direction using a fiber bundle (radius=100 μm) coupled to a spectrometer situated 2 cm away from the sample (Fig. 1). All measurements are taken at an excitation density of $\sim 10^{9}$ cm^{-2} well below the exciton saturation density of 10^{11} cm^{-2}.[8] We have verified that the emission spectra is unchanged and the emission intensity is linear over two orders of magnitude of excitation power so that the enhanced emission is neither a consequence of nonlinear saturation effect nor a final-state stimulation effect.

Figure 2(a) shows the microcavity exciton polariton reso-

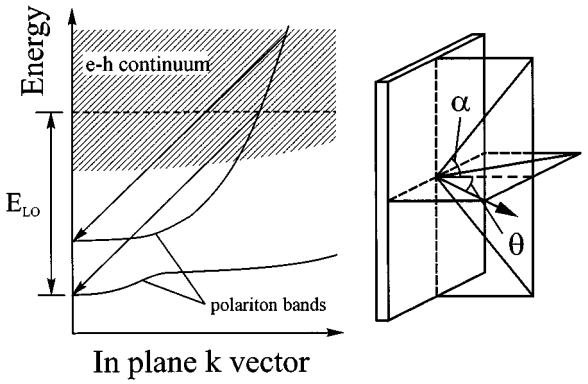

FIG. 1. Schematic diagram showing the resonance enhanced polariton emission by emission of a single LO phonon. The polariton can also thermalize by multiple emissions of acoustic phonons. Also shown is the experimental configuration.

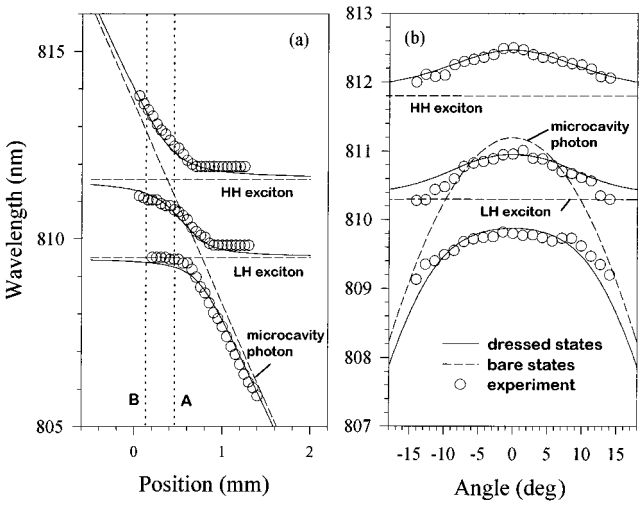

FIG. 2. Anticrossing of LH and HH microcavity polaritons observed as a function of cavity-exciton detuning (a) by varying the excitation position and (b) by changing the observation angle α and fixing the sample position. Solid lines show the theory using an exciton oscillator strength of $f_{\mathrm{HH(LH)}}=28\times10^{-5}$ Å^{-2} (13.2×10^{-5} Å^{-2}). Dashed lines show the energy of the bare excitons and photon states.

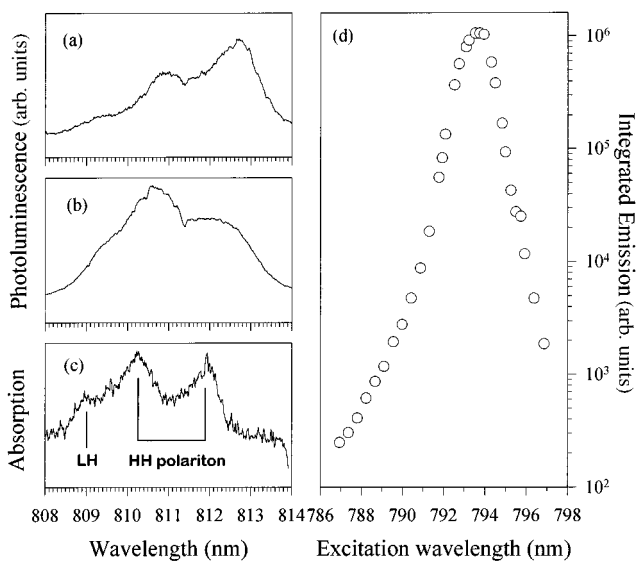

FIG. 3. PL spectra of the HH polariton taken at position A of Fig. 2 when the laser is tuned E_{LO} above the (a) lower-energy and (b) upper-energy HH polariton resonances. (c) Absorption spectra taken at the same sample position. (d) Integrated spectral emission from the upper HH exciton polariton as a function of laser wavelength.

nances for the lowest-order heavy-hole (HH) and light-hole (LH) excitons as a function of sample position, which are taken by the reflectivity measurement. Figure 2(b) shows the angular dispersion[9] of the three polaritons branches at a fixed sample position, which are taken by the photoluminescence (PL) measurement. The resonances are found by fitting reflectivity and PL spectra with superposition of Lorentzians. The solid curves show the theoretical calculations using an extended model from Ref. 10 that takes into account the presence of the LH exciton. The dashed curves show the corresponding bare states with no exciton-photon coupling. The observed HH and LH splittings of 1.5 nm (3 meV) and 1 nm (2 meV) agree well with theoretical values of the oscillator strength for the 1s exciton.[11] In general, the polariton linewidth is a function of exciton-cavity detuning, the bare cavity linewidth, homogeneous linewidth of the bare exciton and the inhomogeneous linewidth of the exciton.

Neglecting polariton effects, the microcavity Fabry-Perot resonance as a function of external (air) incident angle θ is

$$E_{\mathrm{FP}}(\theta)=\frac{\hbar c}{\lambda_0}[1-n^{-2}\sin(\theta)^2]^{-1/2} \tag{1}$$

where n is the effective index of the cavity spacer layer and λ_0 is the resonance vacuum wavelength at the normal direction [the microcavity photon curve in Fig. 2(b)]. We consider the resonance exciton where $E_{\mathrm{FP}}(\theta)=E_{\mathrm{laser}}=E_p(k_\parallel\simeq0)+E_{\mathrm{LO}}$, where E_{laser}, $E_p(k_\parallel\simeq0)$, and E_{LO} are the energies of the excitation laser, $k_\parallel\simeq0$ polariton state and longitudinal-optical phonon, respectively. Figures 3(a)–3(c) shows the PL spectra measured in the normal direction, $\alpha=0$ ($k_\parallel=0$), for position A (Fig. 2) at different excitation laser wavelengths. The resonance condition given by Eq. (1) is maintained for each excitation wavelength by tuning the incident excitation angle $\theta\simeq45°$ to 54°. Experimentally, maximal emission is obtained when the laser is tuned near 33.7 meV $=E_{\mathrm{LO}}$ above the polariton resonances. The value of 33.7 meV indicates that the increase in emission is caused by resonant emission of QW GaAs LO phonon through the Frölich interaction.[12] Figures 3(a) and 3(b) shows the PL for the case where the laser is E_{LO} above the lower- and upper-energy HH exciton polariton at 812.8 nm (1.527 eV) and 810.6 nm (1.531 eV), respectively. Enhanced emission from the polariton state is observed when the excitation laser is E_{LO} larger than the respective polariton energy, showing that one can selectively create a nonequilibrium polariton population simply by tuning the excitation laser. Depending on the laser wavelength, either the upper or lower-energy polariton emission can be dominant. In general, we find that the emission from the LH exciton polariton at 809 nm (1.534 eV) is weak in comparison with the HH exciton polaritons.

Figure 3(c) shows the absorption spectrum at the same sample position. Comparison of Figs. 3(b) and 3(c) shows that the PL is redshifted with respect to the absorption by 0.3 nm (0.6 meV), and this is attributed to the inhomogeneous broadening of the QW exciton. A similar redshift is observed in the PL and absorption measurements shown in Fig. 2. Figure 3(d) shows the spectrally integrated emission from the upper HH polariton state as a function of the excitation wavelength at a fixed sample position while maintaining the resonant excitation condition (1). Experimentally, this is achieved by maximizing the emission in the normal direction by angular tuning. The sample is oriented such that the slight beam displacement caused by angular tuning is along the least tapered direction. The resonant enhancement of the polariton emission by more than three orders of magnitude was observed. By monitoring the spectra, we have carefully checked that the change of emission intensity is not due to an inadvertent change of excitation spot position as the excitation angle is optimized.

The population at the HH exciton polariton with $k_\parallel\simeq0$ is

created by thermalization of a hot electron-hole pair (e-h) with large $k_\parallel$ by multiple acoustic-phonon emission or a single LO-phonon emission. The efficiency in creating a $k_\parallel=0$ polariton by the multiple acoustic phonon emission process is very low since the intermediate states after each emission of an acoustic phonon has a finite probability to emit photons out of the cavity, i.e., most of the photons go to nonradiative decay or to $k_\parallel\neq 0$. We attribute the enhanced polariton emission in the normal direction (over three orders of magnitude compared to the off-resonant excitation) to the elimination of intermediate photon emission associated with the acoustic phonon process and directed to oblique angles ($k_\parallel\neq 0$). The microcavity polariton dispersion ensures that the LO-phonon emission results in a final state with small transverse wave vector. Considering only the LO-phonon emission, the dominant relaxation process is hot electron-hole relaxation to polariton. Initially, a hot electron (e) and hole (h) pair is created. The hot electron-hole pair then emits one LO phonon and forms a polariton (Fig. 1). The e-h continuum state at the polariton branch one E_{LO} above the band bottom is resonantly enhanced by the microcavity. There are two relevant processes involving LO-phonon emission. The first transition process starts from a real energy broadened e-h population, which relaxes to the polariton through LO- phonon emission (hot luminescence). The second is phase conserving and can be described by third-order perturbation theory (Raman process)[13,14] which has a rate

$$I(E,\theta,\alpha)\propto\sum_{i,f}\left|\frac{\langle 0|H_{\mathrm{int}}|i\rangle\langle i|H_{\mathrm{phonon}}|f\rangle\langle f|H'_{\mathrm{int}}|0\rangle}{(E_{\mathrm{laser}}-E_i+i\Gamma_i)(E-E_f+i\Gamma_f)}\right|^2\times\delta(E_{\mathrm{laser}}-E-E_{\mathrm{LO}}) \tag{2}$$

where $H_{\mathrm{int}}=g(a^\dagger b_{e,k}b_{h,-k}+ab^\dagger_{e,k}b^\dagger_{h,-k})$, $H'_{\mathrm{int}}=g'(a'^\dagger C+a'C^\dagger)$, and $H_{\mathrm{phonon}}=\kappa(b^\dagger_{e,k}b^\dagger_{h,-k}BC+b_{e,k}b_{h,-k}B^\dagger C^\dagger)$ are e-h–photon, polariton-photon, and e-h–LO-phonon-polariton interactions, respectively. a, a', $b_{e(h)}$, B, and C are destruction operators for the pump photon, emitted photon, electron (hole), LO phonon, and polariton. g, g', and κ are effective coupling constants that are proportional to the overlap of the wave functions of the quasiparticles. E is the energy of the emitted photon. For the triply resonant case where $E_{\mathrm{laser}}\simeq E_{\mathrm{FP}}(\theta)=E_i$, $E\simeq E_p(k_\parallel=0)=E_f$, and $E_{\mathrm{laser}}\simeq E+E_{\mathrm{LO}}$ and for large cavity-exciton detuning such that only one polariton state is relevant, Eq. (2) simplifies to

$$I(E)\propto\left|\frac{1}{(E_{\mathrm{laser}}-E_{\mathrm{FP}}(\theta)+i\Gamma_{\mathrm{cav}})(E-E_p(k_\parallel\simeq 0)+i\Gamma_p)}\right|^2\times\frac{1}{(E_{\mathrm{laser}}-E-E_{\mathrm{LO}})^2+\Gamma^2} \tag{3}$$

where we replace the δ function with a Lorentzian to account for intermediate state dephasing Γ_i using one effective level $|i\rangle=|$hot electron and hole$\rangle$ and an effective Γ. We note that Eq. (3) describes also the first process, as it contains initial state coupling efficiency (FP transmission), the final-state coupling efficiency (polariton emission), and an intermediate energy broadening in the third term. Γ effectively accounts for both Raman and luminescence intermediate-state broadening which is caused by the finite LO-phonon lifetime and by the broadening of the e-h pair by Coulomb scattering,

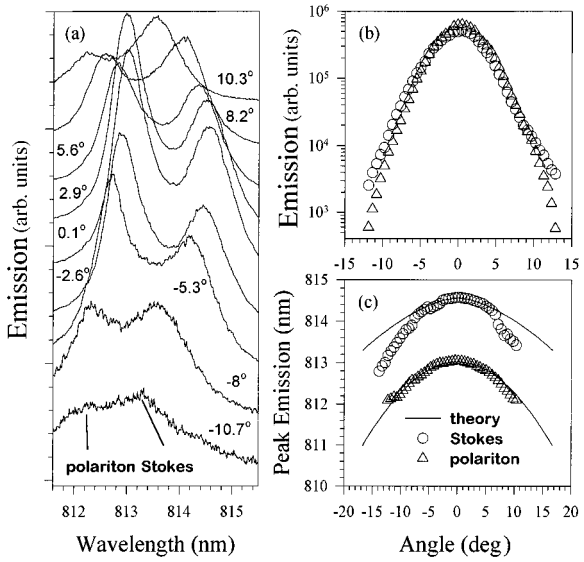

FIG. 4. (a) Spectra taken at different angles α at position B of Fig. 2 at a fixed excitation power and laser wavelength of 797 nm (1.557 eV). (b) The integrated intensity of the polariton (triangle) and LO-phonon peaks (circle) is taken by fitting to Lorentzian as a function of α. (c) The peak positions of the polariton and LO-phonon peaks for different α. Solid line shows the theoretical calculation using the single intermediate state approximation Eq. (3) ($\Gamma=1.7$ meV, $\Gamma_p=1$ meV).

respectively. This is in contrast to the resonant Raman scattering (virtual) in Ref. 4 where $\Gamma\sim 0$ and the linewidth is limited by the LO-phonon linewidth only. In the virtual Raman process, the input photon creates a LO phonon and a output Stokes photon almost instantaneously after its absorption. The lifetime of the LO phonon is of the order of 7 ps (0.05 meV) at 77 K (Ref. 15) and 3.5 ps (0.1 meV) at room temperature[16] and leads to a narrow Stokes line. For bulk polariton, the resonant Raman line had been observed to become indistinct with the PL process at resonance.[17] The enhanced polariton emission shown in Fig. 3(d) occurs when $E_{\mathrm{laser}}=E+E_{\mathrm{LO}}$ and $E=E_p(k_\parallel\simeq 0)$, i.e., when all the denominators in Eq. (3) are minimized (triple resonances), and is similar to the enhanced Raman scattering observed in Ref. 4 where $E_{\mathrm{laser}}=E_S+E_{\mathrm{LO}}$ and $E_{\mathrm{laser}}\simeq E_f(k_\parallel\simeq 0)$. $E=E_S$ is the energy of the LO-phonon line. Equation (3) shows that the peak of the emission is in general a function of E_p and Γ_p of the final polariton state. For the cases, $\Gamma_p\gg\Gamma$, $\Gamma_p=\Gamma$, and $\Gamma_p\ll\Gamma$, the emission peak is located at $E_{\mathrm{peak}}=E_{\mathrm{laser}}-E_{\mathrm{LO}}$, $[E_{\mathrm{laser}}-E_{\mathrm{LO}}+E_p(k_\parallel\simeq 0)]/2$, and $E_p(k_\parallel\simeq 0)$, respectively. Hence, for $\Gamma_p\leqslant\Gamma$ the LO-phonon line position is a strong function of the final polariton energy E_p. This resonance pulling effect is observed from the spectra of the polariton emission and the LO-phonon line measured at different emission angle α.

Figure 4(a) shows the spectra taken at position B (Fig. 2) where the lower HH polariton peak is photonlike, i.e., the photon component of the lower HH polariton is greater than the corresponding exciton component. Note that the data are not taken at the resonant condition given by Eq. (1), but are slightly detuned. By tuning the pump laser wavelength, the LO phonon line can be observed separately from the polariton emission peak to shift from the longer-wavelength side

to the shorter-wavelength side of the polariton peak. The intensity of the separate LO-phonon line can be smaller than or comparable to that of the polariton PL depending on the detuning. For finite detuning, the emission from the polariton peak is primarily caused by the acoustic phonon relaxation process. Figure 4(b) shows the spectrally integrated intensity of the polariton and LO-phonon line as a function of angle α. The value of $\Delta\alpha_{\mathrm{FWHM}}=5°$ (where FWHM is full width at half maximum) agrees well with the emission angle of the microcavity calculated by using the simple relation $\Delta\lambda_{\mathrm{FWHM}}/\lambda_0=(\Delta\alpha_{\mathrm{FWHM}}/2n)^2$ and a measured bare cavity linewidth of 0.25 nm (0.5 meV). This suggests that the width of the emission lobe of the polariton is primarily a function of the cavity reflectivity and geometry and not a function of the polariton population at different $k_\parallel$. Figure 4(c) shows the peak position of the LO-phonon line at different observation angles. The position of the LO-phonon line is strongly dependent on the position of the polariton state for a fixed angle. The solid curve is calculated using Eq. (3) and qualitatively describes the location of the polariton and LO-phonon peaks. Note that this is very different from the polariton process in bulk where there is no conservation of photon momentum along k_z (normal to interface). For the Raman process, the emission spectrum is within a solid angular cone. For a two-dimensional microcavity system, k_z is quantized, and the emission spectrum is highly angular dependent as shown in Fig. 4(c).

In conclusion, the intensity of the microcavity exciton polariton emission can be resonantly enhanced by over three orders of magnitude when the excitation laser is tuned at an energy E_{LO} above the polariton states. The PL shows a nonequilibrium distribution of polariton and allows a clearer identification of the position of the polariton resonances. We have measured the angular PL for the LH and HH polaritons, and the results fit well with theoretical polariton dispersion. Utilization of the LO-phonon emission process allows the efficient population of $k_\parallel=0$ polariton and has potential in application of excitonic light emitting device.

The authors thank T. Norris, H. M. Gibbs, and J. Berger for sending us their work prior to publication. S.P. acknowledges support from the John and Fannie Hertz Foundation and helpful discussions with V. Savona.

[1] T. Norris *et al.*, Phys. Rev. B **50**, 14 663 (1994); B. Deveaud *et al.*, Phys. Rev. Lett. **67**, 2355 (1991).
[2] Y. Yamamoto and R. E. Slusher, Phys. Today **46**, 66 (1993).
[3] K. T. Tsen and H. Morkoç, Phys. Rev. B **38**, 5615 (1988).
[4] A. Fainstein *et al.*, Phys. Rev. Lett. **75**, 3764 (1995).
[5] A. Imamoğlu *et al.*, Phys. Rev. A **53**, 4250 (1996).
[6] C. Weisbuch *et al.*, Phys. Rev. Lett. **69**, 3314 (1992); Y. Yamamoto *et al.*, J. Phys. (France) II **3**, 39 (1993); T. A. Fisher *et al.*, Phys. Rev. B **51**, 2600 (1995); R. Stanley *et al.*, *ibid.* **53**, 10 995 (1996); B. Sermage *et al.*, *ibid.* **53**, 16 516 (1996); G. Khitrova *et al.*, Phys. Rev. Lett. (to be published); J. Bereg *et al.*, Phys. Rev. B **54**, 1975 (1996).
[7] D. S. Citrin, IEEE J. Quantum Electron. **30**, 997 (1994); S. Jorda Phys. Rev. B **51**, 10 185 (1995); V. Savona *et al.*, Solid State Commun. **93**, 733 (1995).
[8] S. Schmitt-Rink *et al.*, Phys. Rev. B **32**, 6601 (1985).
[9] R. Houdre *et al.*, Phys. Rev. Lett. **73**, 2043 (1994).
[10] S. Pau *et al.*, Phys. Rev. B **51**, 7090 (1995); S. Pau *et al.*, *ibid.*, **51**, 14 437 (1995).
[11] L. C. Andreani and A. Pasquarello, Phys. Rev. B **42**, 8928 (1990).
[12] Note that it is shifted from the bulk LO-phonon energy due to the multilayer microcavity structure (see Ref. 4).
[13] A. J. Shields *et al.*, Phys. Rev. B **51**, 17 728 (1995); J. E. Zucker *et al.*, *ibid.* **35**, 2892 (1987).
[14] B. Jusserand and M. Cardona, in *Light Scattering in Solids*, edited by M. Cardona and G. Güntherodt (Springer, Berlin, 1989), Vol. 5.
[15] D. von der Linde, J. Kuhl, and H. Klingenbereg, Phys. Rev. Lett. **44**, 1505 (1980).
[16] J. A. Kash *et al.*, Phys. Rev. Lett. **58**, 1869 (1987).
[17] A. Nakamura and C. Weisbuch, Solid State Commun. **32**, 301 (1979).